Delay Characterization of Rateless Codes in Wireless Ad Hoc Networks

Na Deng*† and Martin Haenggi‡
*School of Information & Communication Engineering, Dalian University of Technology, Dalian, 116024, China
†National Mobile Communications Research Laboratory, Southeast University, Nanjing, 210096, China
‡Dept. of Electrical Engineering, University of Notre Dame, Notre Dame, IN, 46556, USA
Email:*†dengna@dlut.edu.cn, ‡mhaenggi@nd.edu

***Abstract*—Unlike earlier works on rateless codes that mostly considered finite networks or ignored the traffic dynamics, this paper focuses on the end-to-end delay performance of rateless codes in large-scale wireless ad hoc networks with traffic dynamics. Specifically, the end-to-end delay is divided into two parts, namely the packet waiting time before transmission and the transmission time, whose statistical distributions are given by exact results as well as simple yet accurate approximations. This way, the statistics of the end-to-end delay are fully investigated. The proposed analytical framework and the end-to-end performance metric help obtain more insights on the role of scheduling, queueing, and coding scheme in practical networks. The approximations are verified to be effective and reliable through simulations. Overall, the results show the significant benefits of rateless codes relative to the fixed-rate codes in terms of the end-to-end delay performance.**

I. Introduction

Recently, the rapid development of emerging latency-critical applications, such as intelligent manufacturing, remote control, auxiliary driving, and automatic driving, has led to stringent end-to-end delay requirements [1]. The conventional analysis is usually based on queueing theory with a collision model to simplify the physical layer. However, in practical networks, the effect of the interference cannot be accurately modeled merely by a collision since it is related to the channel fluctuations, path loss, as well as the spatial distribution of the network transceivers. Due to its effective characterization of the interference in large-scale wireless networks, stochastic geometry has successfully built a bridge between the queueing dynamics and the signal transmission in the physical layer. In this line of research, the delay performance has been analyzed for various types of wireless networks, such as ad hoc [3], TDMA/ALOHA-based multihop [4], and heterogenous cellular networks [5]. However, since they used fixed-rate codes with constant transmission time, the end-to-end delay was actually measured by the mean queueing delay and its statistics have not been explored in depth.

In regard to the transmission delay, rateless coding has received a widespread attention as an error correction technique due to its capability of adapting both the code construction and the number of parity symbols to time-varying channel conditions [6], which is expected to improve the signal-to-interference ratio (SIR) and reduce the transmission delay. Existing works mostly focus on the benefits of rateless codes in finite wireless networks, and although the authors in [6] and [7] have provided the performance analysis of rateless codes in large-scale ad hoc and cellular networks, the full-buffer assumption, which neglects the queueing dynamics, leads to significant deviations from the actual end-to-end delay performance. In summary, there is so far no comprehensive investigation of the end-to-end performance of rateless codes in large-scale wireless networks considering the impact of the queueing process. We will fill this gap with new analytical results on the statistics of end-to-end delay in wireless ad hoc networks with rateless codes and buffers at transmitters.

Combining the tools from stochastic geometry and queueing theory, we propose an analytical framework with the spatial distribution and the spatio-temporal traffic of transmitters following a homogeneous Poisson point process (PPP) [8] and a Poisson arrival process (PAP), respectively. The end-to-end delay is divided into two parts: the packet waiting time before transmission and the transmission time, where the former is presented by an M/Geo/1 queueing model [9] with random scheduling and the latter is transformed into the decoding time of rateless coding for a packet with fixed-size information. Specifically, we first provide an exact statistical distribution of the packet waiting time using queueing theory and propose an accurate approximation via the effective bandwidth concept [10, 11]. Then we approximate the packet transmission time by simplifying the behavior of the interferers. Based on the analysis for the statistics of the two kinds of delay, the distribution of the end-to-end delay is finally derived. As a benchmark, the end-to-end delay of fixed-rate codes in ad hoc network is also quantified. The approximations are validated to be effective and reliable through simulations, and numerical results also show the significant benefits of rateless codes relative to the fixed-rate codes in terms of the end-to-end delay.

II. System Model

A. Network Model

We consider an interference-limited ad hoc network using rateless codes, where the (potential) transmitters form a homogeneous PPP Φ of density λ with unit transmit power. According to the concept of the frame (or subframe) in 4G and future 5G networks [12], discrete frames are introduced with duration T_{f}. Each transmitter is assumed to have a dedicated receiver at distance r_0 in a random orientation, i.e., the

transceiver pairs form a Poisson bipolar network [8, Def. 5.8]. We consider a receiver at the origin that attempts to receive from an additional transmitter located at $(r_0, 0)$ and it becomes the typical receiver under expectation over the PPP due to Slivnyak's theorem [8, Thm. 8.10]. The standard path loss model $\ell(x) = |x|^{-\alpha}$ with exponent α is adopted to represent the path loss function between transmitter x and the origin. The power fading coefficient associated with transmitter x in frame k is denoted by $h_{x,k}$ which is assumed to be an exponential random variable with $\mathbb{E}(h_{x,k}) = 1$ (Rayleigh fading). In addition, the fading coefficients remain constant over each frame and are spatially and temporally independent.

Each transmitter is assumed to have a buffer of infinite capacity to store the generated packets and to apply the first-input-first-output (FIFO) rule to transmit packets. The packets at different transmitters are generated according to independent PAPs with arrival rate ζ (packets per second), and each packet has K information bits. Specifically, at the beginning of each frame, each node in Φ independently sends its head-of-line packet with probability p if its buffer is not empty. During each transmission, K information bits are encoded by a rateless code and sent via Gaussian symbols incrementally over the channel. At the receiver side, the channel output symbols are collected to decode the K information bits with the rateless decoder. The parity transmission continues until the transmitter receives an acknowledgment (ACK) from the receiver or the frame runs out. When the typical receiver is receiving signals from its transmitter, all the other active transmitters are interferers until they receive their ACK and stop their transmission. Due to the constrained end-to-end latency and the high reliability achieved through the use of rateless codes [7], we assume no retransmission mechanism, i.e., if a packet is not transmitted error-free in one frame, it will be dropped.

B. Delay Characterization

The end-to-end delay of packet transmission is evaluated in two phases: one is the waiting phase where the packet waiting time measures the delay between the time when a packet arrives at the buffer and the time when it starts to be transmitted; the other is the transmission phase where the packet transmission time is either the time to successfully transmit a packet within a frame or the frame length.

1) Packet Waiting Time: Due to the PAP of the packets and the ALOHA scheme, an M/Geo/1 queueing model with arrival rate ζ is adopted to characterize the queueing process at each transmitter, where its service time $T_{\rm sv}$ follows a geometric distribution as

$$\mathbb{P}(T_{\rm sv} = nT_{\rm f}) = (1-p)^{n-1}p,\ n \geq 1. \tag{1}$$

Then the statistics of the sojourn time $T_{\rm sj}$ of a packet in the M/Geo/1 queue can be obtained by those of $T_{\rm sv}$ and the Pollaczek-Khintchine transform equation [9], which will be given in the next section. Denote by $T_{\rm w}$ the waiting time for a given packet. Since each packet is transmitted from the start of each frame and the transmission time does not exceed the current frame length, the packet waiting time is $T_{\rm w} = T_{\rm sj} - T_{\rm f}$.

2) Packet Transmission Time: Thanks to the adoption of rateless codes, the packet transmission time is less than the frame duration unless the packet is dropped. For $k \in \mathbb{N}^+$, let t_k be the starting time of the k-th frame, i.e., $t_k = (k-1)T_{\rm f}$. The instantaneous interference at the typical receiver at time t in frame k is

$$I_k(t) = \sum_{x\in\Phi} \ell(x) h_{x,k} B_{x,k} \mathbf{1}_{Q_{x,k}>0} e_{x,k}(t),\ t_k \leq t < t_{k+1}, \tag{2}$$

where k denotes the k-th frame, $Q_{x,k}$ is the number of packets in the queue of transmitter x, $B_{x,k} = 1$ with probability p (and $B_{x,k} = 0$ otherwise), $e_{x,k}(t) = \mathbf{1}(t_k \leq t \leq t_k + T_{x,k})$ denotes the active state of transmitter x at time t, and $T_{x,k}$ is the packet transmission time between x and its receiver. The nearest-neighbor decoder is adopted to perform minimum Euclidean distance decoding merely based on the desired channel gain, as suggested in [13]. Thus the achievable rate $C_k(t)$ is

$$C_k(t) = W \log_2(1 + \hat{\rm SIR}(t)), \tag{3}$$

where W denotes the bandwidth for information transmission, $\hat{\rm SIR}(t) = \ell(x_0)h_{x_0,k}/\hat{I}_k(t)$ is the time-average received SIR, and $\hat{I}_k(t)$ represents the time-average interference at the typical receiver from t_k up to time t, given by

$$\begin{aligned}\hat{I}_k(t) &= \frac{1}{t-t_k}\int_{t_k}^{t} I_k(\tau){\rm d}\tau \\ &= \sum_{x\in\Phi} \ell(x) h_{x,k} B_{x,k} \mathbf{1}_{Q_{x,k}>0} \eta_{x,k}(t),\ t_k \leq t < t_{k+1},\end{aligned} \tag{4}$$

where

$$\eta_{x,k}(t) = \frac{1}{t-t_k}\int_{t_k}^{t} e_{x,k}(\tau){\rm d}\tau = \min\left\{1, \frac{T_{x,k}}{t-t_k}\right\}. \tag{5}$$

Since each interfering transmitter ceases to interfere with other ongoing transmissions after receiving the ACK signal, $\hat{I}_k(t)$ is a monotonically decreasing function of t within each frame, and thus $C_k(t)$ is monotonically increasing with t. Let $\hat{T}_k$ be the time needed to decode a packet with K information bits in frame k, we have

$$\hat{T}_k = \min\{t : K < t \cdot C_k(t)\}, \tag{6}$$

and the packet transmission time follows as $T_k = \min\{\hat{T}_k, T_{\rm f}\}$.

III. Delay Analysis

In this section, we first give an exact analytical expression and a simple approximation for the complementary cumulative distribution function (CCDF) of the packet waiting time. As for the packet transmission time, since an exact calculation for its CCDF seems infeasible, we then provide an approximation for it by simplifying the behavior of the interferers.

A. Packet Waiting Time Analysis

Since $T_{\rm w} = T_{\rm sj} - T_{\rm f}$, $\mathbb{P}(T_{\rm w} > b) = \mathbb{P}(T_{\rm sj} > b + T_{\rm f})$ and we resort to the derivation of the CCDF for $T_{\rm sj}$ through standard queueing theory. According to the Pollaczek-Khintchine transform equation for the sojourn time [9, Eq. 5.13], the Laplace-Stieltjes transform (LST)[1] of $T_{\rm sj}$ is

$$\mathcal{L}_{T_{\rm sj}}(s) = \frac{(1-\varepsilon)s\mathcal{L}_{T_{\rm sv}}(s)}{s - \zeta[1 - \mathcal{L}_{T_{\rm sv}}(s)]}, \tag{7}$$

where $\varepsilon = \zeta T_{\rm f}/p$ ($\zeta < p/T_{\rm f}$ to guarantee a finite queueing delay) is the probability that the buffer is not empty and $\mathcal{L}_{T_{\rm sv}}(s)$ is the LST of $T_{\rm sv}$, given by

$$\mathcal{L}_{T_{\rm sv}}(s) = \sum_{n=1}^{\infty}(1-p)^{n-1}pe^{-snT_{\rm f}} = \frac{pe^{-sT_{\rm f}}}{1-(1-p)e^{-sT_{\rm f}}}. \tag{8}$$

Through the inverse transform, the CCDF of $T_{\rm w}$ is

$$\mathbb{P}(T_{\rm w} > b) = 1 - \frac{1}{2\pi j}\int_{\gamma-j\infty}^{\gamma+j\infty}\frac{\exp(s(b+T_{\rm f}))}{s}\mathcal{L}_{T_{\rm sj}}(s){\rm d}s, \tag{9}$$

where $j = \sqrt{-1}$ and γ is a real number so that the path of integration is in the region of convergence (ROC) of $\mathcal{L}_{T_{\rm sj}}(s)$. Since the distribution only holds for non-negative $T_{\rm sj}$, the ROC is ${\rm Re}\{s\} > {\rm Re}\{P_0\}$, where P_0 is the solution of equation $\exp(-sT_{\rm f}) = \frac{s-\zeta}{(1-p)s-\zeta}$ of $s \in \mathbb{C}$ with the maximum real part, which can be solved by numerical approaches. Since $s = 0$ is always a solution, the ROC is at most ${\rm Re}\{s\} > 0$.

Although (9) can be evaluated by numerical integration, it requires a careful selection of γ, the range of the numerical integration, which depends on the rate of convergence of the integrand, and its step size. Moreover, the complicated results provide little insight and impose restrictions on further analysis. Therefore, in the following, we provide an approximation to simplify the exact result by means of the effective bandwidth concept [10, 11].

Theorem 1. *The CCDF of the packet waiting time is approximated by*

$$\mathbb{P}(T_{\rm w} > b) \approx \frac{\zeta T_{\rm f}}{p}e^{-\zeta(\exp(u^*)-1)(b+T_{\rm f})+u^*}, \quad b \geq 0, \tag{10}$$

where $u^* > 0$ satisfies

$$\zeta T_{\rm f}(e^{u^*} - 1) + \log\left(pe^{-u^*} + 1 - p\right) = 0. \tag{11}$$

And

$$\mathbb{P}(T_{\rm w} = 0) \approx 1 - \frac{\zeta T_{\rm f}}{p}e^{-\zeta(\exp(u^*)-1)T_{\rm f}+u^*}. \tag{12}$$

Proof: See Appendix A.

Note that $\mathbb{P}(T_{\rm w} = 0)$ represents the probability of the event that a packet arrives at an empty queue and is transmitted immediately[2]. Letting $\mathcal{W}(x)$ be the Lambert W function, which solves $\mathcal{W}(x)e^{\mathcal{W}(x)} = x$, we have $u^* = -\zeta T_{\rm f} - \mathcal{W}\big(-\zeta T_{\rm f}e^{-\zeta T_{\rm f}}\big)$ when $p = 1$. For $p < 1$, from Thm. 1, u^* can be obtained by solving the equation in (11) via numerical techniques. However, the numerical approach usually requires setting an initial range that is provided in the following corollary. It also establishes the uniqueness for the solution of (11).

Corollary 1. *Letting*

$$u_{\rm u} = \frac{1}{\zeta}\Big(-\zeta + 1/T_{\rm f} + \sqrt{(\zeta - 1/T_{\rm f})^2 - 2\zeta\log(p)/T_{\rm f}}\Big),$$
$$u_{\rm l} = \log\Big(\frac{-p + \sqrt{p^2 - 4(1-p)p/(\zeta T_{\rm f})}}{2(1-p)}\Big), \tag{13}$$

the solution of (11) is unique and lies in $(u_{\rm l}, u_{\rm u})$ for $p < 1$.

Proof: Letting $f(u) = \zeta(e^u - 1) + \frac{1}{T_{\rm f}}\log\left(pe^{-u} + 1 - p\right)$, we have $f(0) = 0$, and its first-order derivative is

$$f'(u) = \zeta e^u\Big(1 - \frac{p}{\zeta T_{\rm f}}\frac{1}{pe^u + (1-p)e^{2u}}\Big), \tag{14}$$

which changes from negative to positive as u increases. Accordingly, it means that $f(u)$ decreases at first and increases later, and thus the solution of $f(u) = 0$ is unique for $u > 0$. From the monotonicity of $f(u)$, u^* is larger than the solution of $f'(u) = 0$, and we have a lower bound of u^* as

$$u_{\rm l} = \log\Big(\frac{-p + \sqrt{p^2 - 4(1-p)p/(\zeta T_{\rm f})}}{2(1-p)}\Big). \tag{15}$$

As for an upper bound $u_{\rm u}$ of u^*, we first obtain

$$f(u) > \zeta(u + u^2/2) + \frac{1}{T_{\rm f}}\log(pe^{-u}) = g(u), \tag{16}$$

and $u_{\rm u}$ is the solution of $g(u) = 0$, given by

$$u_{\rm u} = \frac{-(\zeta - 1/T_{\rm f}) + \sqrt{(\zeta - 1/T_{\rm f})^2 - 2\zeta\log(p)/T_{\rm f}}}{\zeta}. \tag{17}$$

■

B. Packet Transmission Time Analysis

Since each transmitter attempts to transmit independently at the beginning of each frame, the achievable rate and the packet transmission time are statistically identical in each frame. Thus, the frame index can be omitted. To characterize the CCDF of the packet transmission time, we note that T and $\hat{T}$ are related as

$$\mathbb{P}(T > b) = \begin{cases} \mathbb{P}(\hat{T} > b) & b \leq T_{\rm f} \\ 0 & b > T_{\rm f}. \end{cases} \tag{18}$$

According to (6), we have

$$\begin{aligned}\mathbb{P}(\hat{T} > b) &= \mathbb{P}\big(K > b \cdot C(b)\big) \\ &\overset{(a)}{=} 1 - \mathbb{E}\Big[\exp\big(-\theta_b r_0^{\alpha}\hat{I}(b)\big)\Big] \\ &= 1 - \mathcal{L}_{\hat{I}(b)}(\theta_b r_0^{\alpha}),\end{aligned} \tag{19}$$

where step (a) follows since h_{x_0} is an exponential distributed variable, $\theta_b = 2^{\frac{K}{bW}} - 1$ and $\mathcal{L}_X(s) = \mathbb{E}_X(\exp(-sX))$ is the Laplace transform (LT) of the random variable X.

[1] Letting $F_X(x)$ be the cumulative distribution function (CDF) of the random variable X, $\mathcal{L}_X(s)$ denotes the LST of X i.e., $\mathcal{L}_X(s) = \int_0^{\infty} e^{-sx}{\rm d}F_X(x)$. If F has a derivative f, the LST of X is the standard Laplace transform.

[2] In this case, to facilitate the analysis, the waiting time before the next frame starts is neglected due to the adoption of M/Geo/1 model, in other words, the packet waiting time in this case is approximated to be zero.

It should be noted that for the packet transmission time analysis, the main technical difficulty lies in the interaction between the interference and the actual transmission time of rateless codes. To be specific, whether the interference is strong or weak largely depends on the number and position of concurrent transmitters, and whether a transmitter is active or not depends on the actual time for a successful transmission of rateless codes, which, in turn, is directly influenced by the interference. Thus, a direct calculation of the exact CCDF of the packet transmission time seems infeasible and we turn to an approximation via the independent-interferer approach [6] where the packet transmission time $\bar{T}_x$ of each interfering transmitter is statistically independent with an identical CCDF $\mathbb{P}(\bar{T} > b)$. Therefore, the interference at the typical receiver in this system is decoupled with the actual packet transmission time, resulting in the following approximation.

Theorem 2. *Let $\mu \triangleq \int_0^{T_\mathrm{f}} \mathbb{P}(\bar{T} > b)\mathrm{d}b$ be the average packet transmission time of interfering transmitters in the independent-interferer system and $\delta \triangleq \frac{2}{\alpha}$. Given that the typical transmitter is active, the CCDF of the packet transmission time T_ii for the typical receiver satisfies*

$$P_\mathrm{ii}^\mathrm{l}(\theta_b) \le \mathbb{P}(T_\mathrm{ii} > b) \le P_\mathrm{ii}^\mathrm{u}(\theta_b),\ b \le T_\mathrm{f}, \tag{20}$$

where

$$P_\mathrm{ii}^\mathrm{u}(\theta_b) = 1 - \exp\Big(-\pi\lambda\zeta T_\mathrm{f}(\min\{1, \frac{\mu}{b}\})^\delta \frac{\pi\delta}{\sin(\pi\delta)}\theta_b^\delta r_0^2\Big), \tag{21}$$

$$P_\mathrm{ii}^\mathrm{l}(\theta_b) = 1 - \exp\Big(-\pi\lambda\zeta\mu\frac{\pi\delta}{\sin(\pi\delta)}\theta_b^\delta r_0^2\Big). \tag{22}$$

Proof: See Appendix B.

From Thm. 2, we can see that the calculation of the CCDF of T_ii requires a known CCDF of $\bar{T}$ to obtain the value of μ. A straightforward choice of such $\bar{T}$ is to use the packet transmission time of the interferers in a dummy-interferer system in which the interfering transmitters continue to transmit "dummy" signal and interfere with other ongoing transmissions after they have received the ACK. Accordingly the interference in such system is an upper bound for the actual one, i.e.,

$$\hat{I}(t) < \sum_{x\in\Phi} \ell(x)h_x B_x \mathbf{1}_{Q_x>0} = I_\mathrm{di}. \tag{23}$$

Furthermore, according to (19), we have

$$\begin{aligned}\mathbb{P}(\hat{T} > b) &< 1 - \mathcal{L}_{I_\mathrm{di}}(\theta_b r_0^\alpha) \\ &= 1 - \exp\Big(-\pi\lambda p\varepsilon\frac{\pi\delta}{\sin(\pi\delta)}s^\delta\Big),\end{aligned} \tag{24}$$

where the LT of I_di is obtained in [8, Sec. 5.1.7]. Then μ can be given by the average packet transmission time of the typical receiver in the dummy-interferer system, i.e.,

$$\mu = T_\mathrm{f} - \int_0^{T_\mathrm{f}} \exp\Big(-\pi\lambda\zeta T_\mathrm{f}\frac{\pi\delta}{\sin(\pi\delta)}\theta_b^\delta r_0^2\Big)\mathrm{d}b. \tag{25}$$

C. End-to-End Delay Analysis

In this section, we characterize the end-to-end delay performance of rateless codes to show the intrinsic connection between the packet waiting delay and the packet transmission delay. To highlight the performance benefits from rateless codes, we also derive the corresponding results for fixed-rate codes.

1) Rateless Codes: The end-to-end delay D is the sum of the packet waiting time T_w and the packet transmission time T, i.e., $D = T_\mathrm{w} + T$. Thus, when $b \le T_\mathrm{f}$, we have

$$\begin{aligned}\mathbb{P}(D>b) = \mathbb{P}(T_\mathrm{w}=0)\mathbb{P}(T>b) \\ +\int_{0^+}^{b}\mathbb{P}(T>b-t)f_{T_\mathrm{w}}(t)\mathrm{d}t + \mathbb{P}(T_\mathrm{w}>b),\end{aligned} \tag{26}$$

and when $b > T_\mathrm{f}$,

$$\mathbb{P}(D>b) = \int_{0^+}^{b}\mathbb{P}(T>b-t)f_{T_\mathrm{w}}(t)\mathrm{d}t + \mathbb{P}(T_\mathrm{w}>b), \tag{27}$$

where $f_{T_\mathrm{w}}(t)$ is the probability density function of T_w. Based on the CCDF of T_w in Thm. 1, we have

$$f_{T_\mathrm{w}}(t) \approx \frac{\zeta^2 T_\mathrm{f}}{p}(e^{u^*}-1)e^{-\zeta(\exp(u^*)-1)(t+T_\mathrm{f})+u^*},\ t>0, \tag{28}$$

and $\mathbb{P}(T > t)$ can be approximated by Thm. 2.

2) Fixed-Rate Codes: When fixed-rate coding is adopted, each transmitter is active during the entire frame. Thus, the packet transmission time is constant, i.e., $T = T_\mathrm{f}$, and the end-to-end delay is $D = T_\mathrm{w} + T_\mathrm{f}$. Due to the continuous transmission in each frame, the interference at the typical receiver is same as that in the dummy-interference system. Hence, the end-to-end delay of fixed-rate codes is

$$\mathbb{P}(D>b) = \begin{cases}\mathbb{P}(T_\mathrm{w} > b - T_\mathrm{f}) & b \ge T_\mathrm{f} \\ 1 & b < T_\mathrm{f}.\end{cases} \tag{29}$$

IV. Numerical Results

In this section, we give some numerical results to demonstrate the performance of rateless codes discussed above in wireless ad hoc networks, where $\lambda = 1\times10^{-3}\mathrm{m}^{-2}$, $r_0 = 2$ m, $\alpha = 4$, $T_\mathrm{f} = 0.1$ms, $p = 0.5$, $W = 1$MHz, $\zeta = 400$ packets/s, and $K = 160$ bits are the default values.

Fig. 1 plots the CCDFs of the packet waiting time T_w for different T_f, p and ζ, where the exact and approximative results are obtained via the inverse Laplace transform in (9) and Thm. 1, respectively. It is observed that the approximations derived from the effective bandwidth concept match the exact results extremely well under different parameter settings, which substantially enhances the analytical tractability. It is also seen that the logarithmic form of $\mathbb{P}(T_\mathrm{w} > b)$ decays linearly as b increases with the slope $\zeta(e^{u^*}-1)$. Consisted with the result in (12), $\mathbb{P}(T_\mathrm{w} > b) \neq 1$ as $b \to 0$ since $\mathbb{P}(T_\mathrm{w} = 0) > 0$. In addition, the packet waiting time becomes longer as ζ or T_f increases or as p decreases. The reason lies in that the packet waiting time depends on the queue length in the buffer, and a larger ζ will contribute to the packet backlog in the queue, while a smaller T_f or a larger p will increase the service rate and hence the packets leave the queue faster.

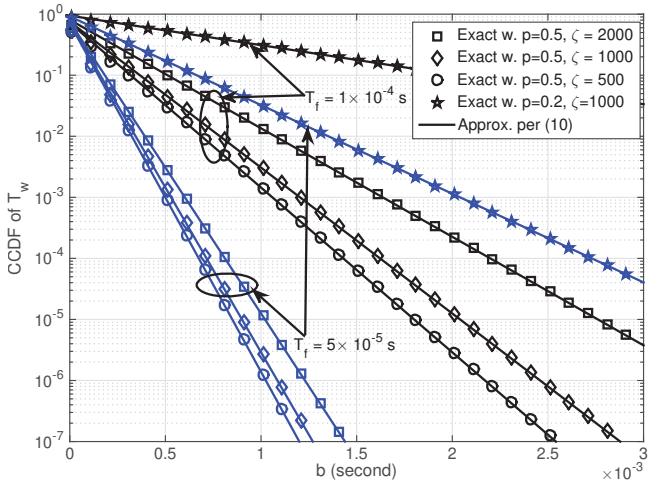

Fig. 1. Validating the approximation for the CCDF of the packet waiting time.

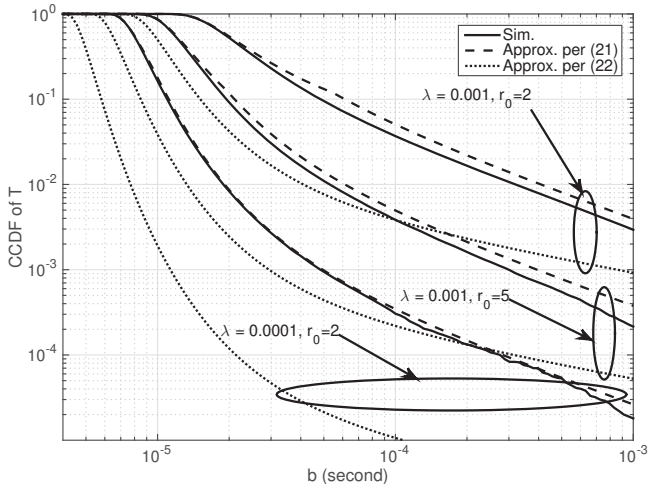

Fig. 2. Validating the approximation for the CCDF of the packet transmission time.

Fig. 2 illustrates the CCDFs of the packet transmission time T with analytical approximations as well as simulation results for different node densities λ and link distances between transceiver r_0. It is seen that the upper bound of the packet transmission time T_{ii} in the independent-interferer system provides a close approximation to the actual transmission time. Furthermore, we observe that the approximation accuracy is higher when the node density is small and is hardly affected by the link distance. It is because the intermediate quantity of the average packet transmission time μ of interferers evaluated through the dummy-interferer approach is closely related to the node density, and its deviation from the exact result of rateless codes would become obvious in denser networks. In other words, the node density plays an important role in determining the approximation accuracy of the dummy-interferer approach.

Fig. 3 shows the CCDFs of the end-to-end delay D using rateless codes in comparison with fixed-rate codes. We observe that rateless coding always achieves a lower end-to-end delay than fixed-rate coding, demonstrating the benefit of rateless

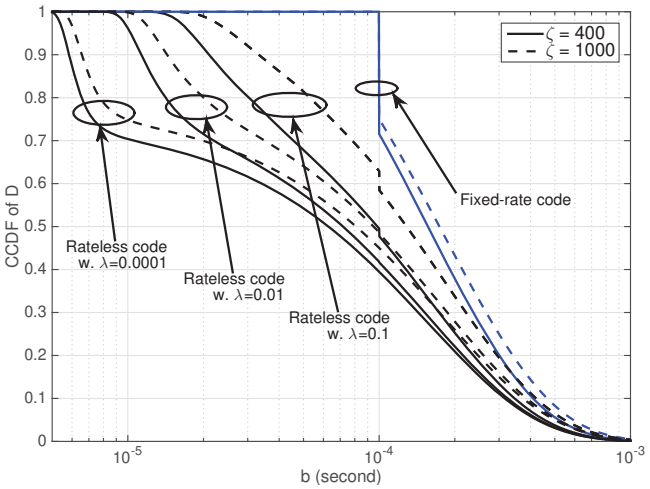

Fig. 3. The end-to-end delay distributions for different λ and ζ.

codes in terms of the transmission delay. In addition, as the node density decreases, the delay advantage of rateless codes over fixed-rate codes is more significant since the node density does not affect the transmission time of fixed-rate codes. Since the end-to-end delay is composed of the packet waiting delay and the transmission delay, a larger ζ and λ result in a longer end-to-end delay because the former contributes to the packet backlog and the latter causes more severe interference.

V. Conclusions

In this paper, we proposed a general framework for the end-to-end delay analysis of rateless codes in wireless ad hoc networks where both the spatial distribution of transmitters and traffic dynamics are incorporated. We investigated the end-to-end delay by dividing it into two parts, namely, the packet waiting time and transmission time, and then provided analytical results including exact expressions and tractable approximations for their statistical distributions. Through comparison with Monte Carlo simulations, the approximations turn to be matching the actual distributions well. Moreover, it is found that the queueing delay is affected by several parameters, such as the frame length, the arrival rate of packets, etc., while the transmission delay is mainly affected by the node density which has a close influence on the interference and, in turn, the number of the parity symbols in rateless coding. Given the statistics of the queueing and transmission delay, the end-to-end delay of rateless codes is quantified with a comparison of fixed-rate codes which highlights the significant benefits in lowering the end-to-end delay, especially when the delay requirement is less than the frame length.

Acknowledgment

The work of N. Deng has been supported by National Natural Science Foundation of China (61701071), the China Postdoctoral Science Foundation (2017M621129), the open research fund of National Mobile Communications Research Laboratory, Southeast University (No. 2019D03), the Fundamental Research Funds for the Central Universities

(DUT16RC(3)119), and the work of M. Haenggi has been supported by the U.S. NSF (grant CCF 1525904).

APPENDIX A
PROOF OF THEOREM 1

Proof: Using the concept of effective bandwidth and capacity in [10, 11], the distributions of the steady-state queue length $Q(\infty)$ and the queueing delay $D_{\rm q}(\infty)$ can be asymptotically approximated. Denote by $A(t)$ and $S(t)$ the total number of packets reaching and leaving the buffer in t time instants, respectively. We first obtain the asymptotic log-moment generating functions of the arrival and service processes, respectively, given by

$$\begin{aligned}\Lambda_A(u) &= \lim_{t\to\infty}\frac{1}{t}\log\mathbb{E}\left[e^{uA(t)}\right]\\ &= \zeta(e^u-1),\end{aligned} \tag{30}$$

and

$$\begin{aligned}\Lambda_S(u) &= \lim_{N\to\infty}\frac{1}{NT_{\rm f}}\log\mathbb{E}\left[e^{uS(NT_{\rm f})}\right]\\ &= \frac{1}{T_{\rm f}}\log(pe^u+1-p).\end{aligned} \tag{31}$$

Then, the effective bandwidth of the arrival process is $E(u)=\Lambda_A(u)/u$. Accordingly, the violation probabilities of the steady-state queueing length and the queueing delay under small threshold can be accurately approximated by

$$\begin{aligned}&\mathbb{P}(Q(\infty)>Q_{\rm th})\approx\mathbb{P}(Q(\infty)>0)\exp(-u^*Q_{\rm th}),\\ &\mathbb{P}(D_{\rm q}(\infty)>D_{\rm th})\approx\mathbb{P}(Q(\infty)>0)\exp(-u^*E(u^*)D_{\rm th}),\end{aligned} \tag{32}$$

where $\mathbb{P}(Q(\infty)>0)=\zeta T_{\rm f}/p$ is the probability that the buffer is not empty, and $u^*>0$ is the decay rate of the tail distribution of the queue length, satisfying $\Lambda_A(u^*)+\Lambda_S(-u^*)=0$. From (32), these two violation probabilities are equivalent by letting $Q_{\rm th}=E(u^*)D_{\rm th}$. For a given packet, its sojourn time is its queueing delay plus its service time, which is equivalent to the queueing delay of a packet with an extra one before it. Therefore, the CCDF of the packet waiting time is

$$\begin{aligned}\mathbb{P}(T_{\rm w}>b) &= \mathbb{P}(T_{\rm sj}>b+T_{\rm f})\\ &\approx \mathbb{P}(Q(\infty)+1>(b+T_{\rm f})E(u^*))\\ &\approx \frac{\zeta T_{\rm f}}{p}\exp\big(-u^*(b+T_{\rm f})E(u^*)+u^*\big).\end{aligned} \tag{33}$$

■

APPENDIX B
PROOF OF THEOREM 2

Proof: According to (19), we have

$$\mathbb{P}(T_{\rm ii}>b)=1-\mathcal{L}_{\bar I(b)}(\theta_b r_0^\alpha), \tag{34}$$

where $\bar I(b)=\sum_{x\in\tilde\Phi}\ell(x)h_xB_x\mathbf{1}_{Q_x>0}\bar\eta_x(b)$, $0<b\le T_{\rm f}$ and $\bar\eta_x(b)=\min\{1,\tilde T_x/b\}$. The LT of $\bar I(b)$ is given similarly in [8, Sec. 5.1.7] as

$$\begin{aligned}\mathcal{L}_{\bar I(b)}(s) &= \mathbb{E}\Big[\prod_{x\in\Phi}\Big(1-p\varepsilon+p\varepsilon e^{-s\ell(x)h_x\bar\eta_x(b)}\Big)\Big]\\ &= \exp\Big(-2\pi\lambda p\varepsilon\int_0^\infty\mathbb{E}_{h,\bar\eta(t)}\big[1-e^{-sh\bar\eta(b)r^{-\alpha}}\big]r{\rm d}r\Big)\\ &= \exp\Big(-\pi\lambda p\varepsilon\mathbb{E}(\bar\eta(b)^\delta)\frac{\pi\delta}{\sin(\pi\delta)}s^\delta\Big),\end{aligned} \tag{35}$$

where $\mathbb{E}(\bar\eta(b)^\delta)$ performs the expectation over the packet transmission time $\bar T$ of the interfering transmitters. By inserting $\mathcal{L}_{\bar I(b)}$ into (34), we have

$$\mathbb{P}(T_{\rm ii}>b)=1-\exp\Big(-\pi\lambda p\varepsilon\mathbb{E}(\bar\eta(b)^\delta)\frac{\pi\delta}{\sin(\pi\delta)}\theta_b^\delta r_0^2\Big). \tag{36}$$

Letting $g(\bar T)=\big[\min\{1,\bar T/b\}\big]^\delta$, we have $\mathbb{E}(\bar\eta(b)^\delta)=\mathbb{E}[g(\bar T)]$. The concavity of $g(\bar T)$ can be verified easily by its 2nd derivative

$$\frac{{\rm d}^2g(\bar T)}{{\rm d}^2\bar T}=\begin{cases}\delta(\delta-1)\bar T^{\delta-2}/b^\delta & \bar T\le b\\ 0 & b<\bar T\le T_{\rm f},\end{cases} \tag{37}$$

which shows that $g^{(2)}(\bar T)\le 0$ for $\bar T\in[0,T_{\rm f}]$. Hence, we have $\mathbb{E}[g(\bar T)]\le g(\mathbb{E}(\bar T))=\big[\min\{1,\mu/b\}\big]^\delta$ and $\mathbb{E}[g(\bar T)]\ge\mu/T_{\rm f}$ due to

$$g(\bar T)\ge\Big(1-\frac{\bar T}{T_{\rm f}}\Big)g(0)+\frac{\bar T}{T_{\rm f}}g(T_{\rm f})=\frac{\bar T}{T_{\rm f}}, \tag{38}$$

The final results are obtained by substituting the two bounds of $\mathbb{E}[g(\bar T)]$ in (36). ■

REFERENCES

[1] A. Osseiran, F. Boccardi, V. Braun *et al.*, "Scenarios for 5G mobile and wireless communications: the vision of the METIS project," *IEEE Communications Magazine*, vol. 52, no. 5, pp. 26–35, May 2014.

[2] Y. Zhong, M. Haenggi, F. Zheng, W. Zhang, T. Q. S. Quek, and W. Nie, "Toward a tractable delay analysis in ultra-dense networks," *IEEE Communications Magazine*, vol. 55, no. 12, pp. 103–109, Dec. 2017.

[3] K. Stamatiou and M. Haenggi, "Random-access Poisson networks: Stability and delay," *IEEE Communications Letters*, vol. 14, no. 11, pp. 1035–1037, Nov. 2010.

[4] ——, "Delay characterization of multihop transmission in a Poisson field of interference," *IEEE/ACM Transactions on Networking*, vol. 22, no. 6, pp. 1794–1807, Dec. 2014.

[5] Y. Zhong, T. Q. S. Quek, and X. Ge, "Heterogeneous cellular networks with spatio-temporal traffic: Delay analysis and scheduling," *IEEE Journal on Selected Areas in Communications*, vol. 35, no. 6, pp. 1373–1386, Jun. 2017.

[6] A. Rajanna and M. Haenggi, "Enhanced cellular coverage and throughput using rateless codes," *IEEE Transactions on Communications*, vol. 65, no. 5, pp. 1899–1912, May 2017.

[7] A. Rajanna, I. Bergel, and M. Kaveh, "Performance analysis of rateless codes in an ALOHA wireless ad hoc network," *IEEE Transactions on Wireless Communications*, vol. 14, no. 11, pp. 6216–6229, Nov. 2015.

[8] M. Haenggi, *Stochastic geometry for wireless networks*. Cambridge University Press, 2012.

[9] J. N. Daigle, *Queueing theory with applications to packet telecommunication*. Springer Science & Business Media, 2005.

[10] D. Wu and R. Negi, "Effective capacity: a wireless link model for support of quality of service," *IEEE Transactions on Wireless Communications*, vol. 2, no. 4, pp. 630–643, Jul. 2003.

[11] S. Akin and M. Fidler, "A method for cross-layer analysis of transmit buffer delays in message index domain," *IEEE Transactions on Vehicular Technology*, vol. 67, no. 3, pp. 2698–2712, Mar. 2018.

[12] 3GPP, "Evolved universal terrestrial radio access (E-UTRA) physical channels and modulation (Release 15)," 3rd Generation Partnership Project (3GPP), Technical Specification (TS) 36.211, Jun. 2018, version 15.2.0.

[13] A. Lapidoth, "Nearest neighbor decoding for additive non-Gaussian noise channels," *IEEE Transactions on Information Theory*, vol. 42, no. 5, pp. 1520–1529, Sept. 1996.